



## Vibrations Of A Rotating Disk Under Perpendicular Spacefixed Forces

Mertol TUFEKCI<sup>1,\*</sup> , Omer Ekim GENEL<sup>1</sup> , Hilal KOC<sup>1</sup> , Olcay OLDAC<sup>1</sup> , Ekrem TUFEKCI<sup>1</sup> 

<sup>1</sup>Istanbul Technical University, Department of Mechanical Engineering, 34437, Istanbul, Turkey

### Article Info

Received: 02/02/2018

Accepted: 03/09/2018

### Keywords

Rotating disk  
Spacefixed load  
Galerkin method  
Forced vibration

### Abstract

In this study, forced vibration of a rotating disk is investigated. The disk is clamped at the inner and free at the outer circumferences. A time varying excitation force is applied to a spacefixed point on the disk surface perpendicularly. The presence of multiple excitation forces is also considered in the paper. These forces can be applied to any spacefixed point on the disk surface. The disk is modelled as a thin plate and the Galerkin method is used to analyze the forced vibration characteristics of the rotating disk. Power spectral density diagrams of the forced vibrations with both one and multiple excitation forces are plotted.

## 1. INTRODUCTION

Investigations of rotating and non-rotating disks have long background in engineering sciences. It is obvious that studies about rotating disks are in parallel with industrial needs, like turbines, rotating cutting saws, gears, grinding wheels, etc. In recent years, with the development in informatics industry, it is observed that there is an increasing research trend on rotating disks, especially in data storage devices area.

In the first studies, disks were modeled as thin plates by using linear elasticity theory [1,2]. Studies about vibrational characteristics of disks were based on determining natural frequencies and mode shapes [3-11]. On the other hand, in rotating case, it is very difficult to obtain an analytical solution. Kirkhope and Wilson [3] developed a numerical solution based on finite element approach for axisymmetric disks by executing vibration and stress analyses. In analytical studies, solutions for rotating case were obtained by using Rayleigh-Ritz, Galerkin and Lagrange methods [7-9].

In the literature, it is observed there are two different methods for the investigations about forced vibration of rotating disks. In the first approach, it is assumed that excitation force, which exerts on the disk, moves when the disk does not [12,13]. In that approach, the solution is obtained when stresses, which are produced by rotation movement, are neglected. In the second approach, it is assumed that disk rotates and under the presence of rotation related stresses in the equation of motion, the solution is obtained [14,15]. Also, some studies investigate the dynamic response of rotating disks under prescribed forced displacement excitations [16,17].

In addition, not only vibrations but also stabilities of disks are affected by the rotation movement. The critical speed and stability analyses are also studied both analytically and numerically [18-21].

One of the most accurate examples of a rotating disk under perpendicular spacefixed force is a hard disk. Since it is thought that the axial modes are more dominant, a study which investigates the axial response was presented by Jiang et al. [22]. In addition, disk-read/write head interactions were also modelled both

\*Corresponding author, e-mail: tufekcime@itu.edu.tr

analytically and numerically [23-24]. Also, thanks to numerical and experimental dynamic analyses of harddisk drives under operating conditions, the dynamic characteristics of these systems were determined efficiently [25]. In recent studies, tranverse nonlinear vibration analysis was carried out in the presence of rotating concentrated load by Zhang and Yang [26]. They used clamped-free boundary conditions and utilized the method of multiple scales to solve nonlinear equations. Younesian et al. [27] conducted a research about vibrational characteristics of circular plates by considering rotating loads at the outer edge. They used the Galerkin method and obtained closed-form solution. Norouzi and Younesian [28] investigated the forced vibration characteristics of a rotating disk in the presence of concentrated force. They used the Galerkin method to obtain the solution and examined the response by using both fixed and rotary frames.

In this work, the solution is obtained assuming that the disk rotates and the disk flexibility is taken into consideration. The flexibility of shaft is neglected. When the disk rotates, the forced vibration of disk is examined in the existence of perpendicular spacefixed forces. It is thought that this examination can be a model for harddisk and read/write head interactions. For this purpose, the Galerkin method is used to obtain the solution. In that method, an approximate function which satisfies boundary conditions is chosen and it is substituted into the equation of motion. With the help of this solution, power spectral density diagrams are obtained. The effects of the harmonic forces, which are applied on the arbitrary points of the disk with a specific excitation frequencies, on the amplitudes of some modes are investigated. It is observed that these forces can decrease the amplitude values for some specific cases. Thus, it has shown that the undesired vibrational effects can be eliminated by using a well-designed force system.

## 2. EQUATIONS AND FORMULATION

In spacefixed coordinate system, the equation of motion of a rotating disk under perpendicular distributed force can be written as [17];

$$D \left( \frac{\partial^2}{\partial r^2} + \frac{1}{r} \frac{\partial}{\partial r} + \frac{1}{r^2} \frac{\partial^2}{\partial \psi^2} \right)^2 w + \rho h \left( \frac{\partial^2 w}{\partial t^2} + 2\Omega \frac{\partial^2 w}{\partial \psi \partial t} + \Omega^2 \frac{\partial^2 w}{\partial \psi^2} \right) - \frac{h}{r} \left[ \frac{\partial}{\partial r} \left( \sigma_r r \frac{\partial w}{\partial r} \right) + \frac{\sigma_\psi}{r} \frac{\partial^2 w}{\partial \psi^2} \right] = p(r, \psi, t) \quad (1)$$

Here,  $w$  is the transverse displacement of disk,  $D = Eh^3/[12(1 - \nu^2)]$  is the bending rigidity of the disk ( $\nu$ : Poisson's ratio of the disk material),  $\sigma_r$  and  $\sigma_\psi$  are the radial and tangential stresses which are caused by rotation,  $h$  and  $\Omega$  are the thickness of disk and the rotational speed of disk,  $(r, \psi)$  represent the spacefixed coordinates. Also,  $p(r, \psi, t)$  is variable distributed force which is applied on the disk surface perpendicularly.

The transverse displacement function of the disk can be selected as below:

$$w(r, \psi, t) = \sum_{n=0}^N \sum_{m=0}^M \eta_{mn}(t) R_{mn}(r) \sin(n\psi - \omega_{mn}t) \quad (2)$$

In this equation, sinusoidal term can be written explicitly:

$$w(r, \psi, t) = \sum_{n=0}^N \sum_{m=0}^M [\eta_{mn}(t) \cos \omega_{mn}t \sin n\psi - \eta_{mn}(t) \sin \omega_{mn}t \cos n\psi] R_{mn}(r) \quad (3)$$

Here, in order to express this equation in a simpler form, the abbreviations below are used;

$$q_{mn}^s(t) = \eta_{mn}(t) \cos \omega_{mn}t ; \quad q_{mn}^c(t) = -\eta_{mn}(t) \sin \omega_{mn}t \quad (4)$$

So, Equation (3) can be written as;

$$w(r, \psi, t) = \sum_{n=0}^N \sum_{m=0}^M [q_{mn}^s(t) \sin n\psi + q_{mn}^c(t) \cos n\psi] R_{mn}(r) \tag{5}$$

This equation and its derivatives are substituted into the Equation (1). Thus, the equation of motion is obtained as;

$$\begin{aligned} \sum_{n=0}^N \sum_{m=0}^M \left\{ D \left( \frac{\partial^4 R_{mn}(r)}{\partial r^4} + \frac{2}{r} \frac{\partial^3 R_{mn}(r)}{\partial r^3} - \frac{1 + 2n^2}{r^2} \frac{\partial^2 R_{mn}(r)}{\partial r^2} + \frac{1 + 2n^2}{r^3} \frac{\partial R_{mn}(r)}{\partial r} + \frac{n^4 - 4n^2}{r^4} R_{mn}(r) \right) \right. \\ \left. - \frac{h}{r} \left[ \sigma_r r \frac{\partial^2 R_{mn}(r)}{\partial r^2} + \left( \frac{\partial \sigma_r}{\partial r} r + \sigma_r \right) \frac{\partial R_{mn}(r)}{\partial r} \right] \right. \\ \left. - \frac{n^2}{r} \sigma_\psi R_{mn}(r) \right\} \cdot [q_{mn}^s(t) \sin n\psi + q_{mn}^c(t) \cos n\psi] \\ + \rho h ([\ddot{q}_{mn}^s(t) \sin n\psi + \ddot{q}_{mn}^c(t) \cos n\psi] + 2\Omega n [\dot{q}_{mn}^s(t) \cos n\psi - \dot{q}_{mn}^c(t) \sin n\psi] \\ - \Omega^2 n^2 [q_{mn}^s(t) \sin n\psi + q_{mn}^c(t) \cos n\psi]) R_{mn}(r) \Big\} = p(r, \psi, t) \tag{6} \end{aligned}$$

The term,  $F_{mn}$ , is introduced as below:

$$\begin{aligned} F_{mn} = D \left( \frac{\partial^4 R_{mn}(r)}{\partial r^4} + \frac{2}{r} \frac{\partial^3 R_{mn}(r)}{\partial r^3} - \frac{1 + 2n^2}{r^2} \frac{\partial^2 R_{mn}(r)}{\partial r^2} + \frac{1 + 2n^2}{r^3} \frac{\partial R_{mn}(r)}{\partial r} + \frac{n^4 - 4n^2}{r^4} R_{mn}(r) \right) \\ - \frac{h}{r} \left[ \sigma_r r \frac{\partial^2 R_{mn}(r)}{\partial r^2} + \left( \frac{\partial \sigma_r}{\partial r} r + \sigma_r \right) \frac{\partial R_{mn}(r)}{\partial r} - \frac{n^2}{r} \sigma_\psi R_{mn}(r) \right] \tag{7} \end{aligned}$$

Substituting this abbreviation into Equation (6) gives:

$$\begin{aligned} \sum_{n=0}^N \sum_{m=0}^M \left\{ [F_{mn} q_{mn}^s(t) + \rho h (\ddot{q}_{mn}^s(t) - 2\Omega n \dot{q}_{mn}^c(t) - \Omega^2 n^2 q_{mn}^s(t)) R_{mn}(r)] \sin n\psi + [F_{mn} q_{mn}^c(t) \right. \\ \left. + \rho h (\ddot{q}_{mn}^c(t) + 2\Omega n \dot{q}_{mn}^s(t) - \Omega^2 n^2 q_{mn}^c(t)) R_{mn}(r)] \cos n\psi \right\} = p(r, \psi, t) \tag{8} \end{aligned}$$

Dividing both sides with  $\rho h$  gives the following equation;

$$\begin{aligned} \sum_{n=0}^N \sum_{m=0}^M \left\{ \left[ \ddot{q}_{mn}^s(t) (R_{mn}(r) - 2\Omega n \dot{q}_{mn}^c(t) R_{mn}(r) - \Omega^2 n^2 q_{mn}^s(t) R_{mn}(r) + \frac{F_{mn}}{\rho h} q_{mn}^s(t)) \right] \sin n\psi + \left[ \ddot{q}_{mn}^c(t) R_{mn}(r) \right. \right. \\ \left. \left. + 2\Omega n \dot{q}_{mn}^s(t) R_{mn}(r) - \Omega^2 n^2 q_{mn}^c(t) R_{mn}(r) + \frac{F_{mn}}{\rho h} q_{mn}^c(t) \right] \cos n\psi \right\} = \frac{p(r, \psi, t)}{\rho h} \tag{9} \end{aligned}$$

To get the solution, Galerkin method is used. For this purpose, the weighted residual function is built and solved.

$$\begin{aligned} \int_{R_i}^{R_o} \int_0^{2\pi} \sum_{n=0}^N \sum_{m=0}^M \left\{ \left[ \ddot{q}_{mn}^s(t) R_{mn}(r) - 2\Omega n \dot{q}_{mn}^c(t) R_{mn}(r) - \Omega^2 n^2 q_{mn}^s(t) R_{mn}(r) + \frac{F_{mn}}{\rho h} q_{mn}^s(t) \right] \sin n\psi \right. \\ \left. + \left[ \ddot{q}_{mn}^c(t) R_{mn}(r) + 2\Omega n \dot{q}_{mn}^s(t) R_{mn}(r) - \Omega^2 n^2 q_{mn}^c(t) R_{mn}(r) \right. \right. \\ \left. \left. + \frac{F_{mn}}{\rho h} q_{mn}^c(t) \right] \cos n\psi \right\} \cdot R_{sn}(r) [q_{sn}^s(t) \sin n\psi + q_{sn}^c(t) \cos n\psi] r d\psi dr \\ = \frac{1}{\rho h} \int_{R_i}^{R_o} \int_0^{2\pi} p(r, \psi, t) R_{sn}(r) [q_{sn}^s(t) \sin n\psi + q_{sn}^c(t) \cos n\psi] r d\psi dr \tag{10} \end{aligned}$$

If the order of the integration and summation is changed, the following is obtained after some arrangements;

$$\begin{aligned}
 & \sum_{n=0}^N \sum_{m=0}^M \left\{ \left( \left( \ddot{q}_{mn}^s(t) - 2\Omega n \dot{q}_{mn}^c(t) - \Omega^2 n^2 q_{mn}^s(t) \right) \int_{R_i}^{R_o} R_{mn}(r) R_{sn}(r) r dr \right. \right. \\
 & \quad + q_{mn}^s(t) \int_{R_i}^{R_o} \frac{F_{mn}}{\rho h} R_{sn}(r) r dr \left. \right) \int_0^{2\pi} \sin n\psi \cos n\psi d\psi \\
 & \quad + \left[ \left( \dot{q}_{mn}^c(t) + 2\Omega n \dot{q}_{mn}^s(t) - \Omega^2 n^2 q_{mn}^c(t) \right) \int_{R_i}^{R_o} R_{mn}(r) R_{sn}(r) r dr \right. \\
 & \quad + q_{mn}^c(t) \int_{R_i}^{R_o} \frac{F_{mn}}{\rho h} R_{sn}(r) r dr \left. \right] \int_0^{2\pi} \cos^2 n\psi d\psi \Big) q_{sn}^c(t) \\
 & \quad + \left( \left( \ddot{q}_{mn}^s(t) - 2\Omega n \dot{q}_{mn}^c(t) - \Omega^2 n^2 q_{mn}^s(t) \right) \int_{R_i}^{R_o} R_{mn}(r) R_{sn}(r) r dr \right. \\
 & \quad + q_{mn}^s(t) \int_{R_i}^{R_o} \frac{F_{mn}}{\rho h} R_{sn}(r) r dr \left. \right) \int_0^{2\pi} \sin^2 n\psi d\psi \\
 & \quad + \left[ \left( \dot{q}_{mn}^c(t) + 2\Omega n \dot{q}_{mn}^s(t) - \Omega^2 n^2 q_{mn}^c(t) \right) \int_{R_i}^{R_o} R_{mn}(r) R_{sn}(r) r dr \right. \\
 & \quad + q_{mn}^c(t) \int_{R_i}^{R_o} \frac{F_{mn}}{\rho h} R_{sn}(r) r dr \left. \right] \int_0^{2\pi} \sin n\psi \cos n\psi d\psi \Big) q_{sn}^s(t) \Big\} \\
 & = \frac{1}{\rho h} \left[ \int_{R_i}^{R_o} \int_0^{2\pi} p(r, \psi, t) R_{sn}(r) r \cos n\psi d\psi dr q_{sn}^c(t) \right. \\
 & \quad \left. + \int_{R_i}^{R_o} \int_0^{2\pi} p(r, \psi, t) R_{sn}(r) r \sin n\psi d\psi dr q_{sn}^s(t) \right]
 \end{aligned} \tag{11}$$

If the following definitions are used;

$$\int_{R_i}^{R_o} R_{mn}(r) R_{sn}(r) r dr = \Gamma_{smn} \tag{12}$$

$$\frac{1}{\rho h} \int_{R_i}^{R_o} F_{mn}(r) R_{sn}(r) r dr = \phi_{smn} \tag{13}$$

Equation (11) can be rewritten as follows;

$$\begin{aligned}
 & \sum_{n=0}^N \sum_{m=0}^M \left\{ \left( \left[ \left( \dot{q}_{mn}^c(t) + 2\Omega n \dot{q}_{mn}^s(t) - \Omega^2 n^2 q_{mn}^c(t) \right) \Gamma_{smn} + q_{mn}^c(t) \phi_{smn} \right] \int_0^{2\pi} \cos^2 n\psi d\psi \right) q_{sn}^c(t) \right. \\
 & \quad + \left( \left[ \left( \ddot{q}_{mn}^s(t) - 2\Omega n \dot{q}_{mn}^c(t) - \Omega^2 n^2 q_{mn}^s(t) \right) \Gamma_{smn} + q_{mn}^s(t) \phi_{smn} \right] \int_0^{2\pi} \sin^2 n\psi d\psi \right) q_{sn}^s(t) \Big\} \\
 & = \frac{1}{\rho h} \left[ \int_{R_i}^{R_o} \int_0^{2\pi} p(r, \psi, t) R_{sn}(r) r \cos n\psi d\psi dr q_{sn}^c(t) \right. \\
 & \quad \left. + \int_{R_i}^{R_o} \int_0^{2\pi} p(r, \psi, t) R_{sn}(r) r \sin n\psi d\psi dr q_{sn}^s(t) \right]
 \end{aligned} \tag{14}$$

Here, it is clear that this equation has two different characteristics for  $n=0$  and  $n \neq 0$ . In this study, the coefficients are arranged for  $n \neq 0$ . By arranging the coefficients of  $q_{mn}^c(t)$  and  $q_{mn}^s(t)$ , the equations can be represented as second order linear differential equations. In matrix notation, for every  $n$  value, it can be rewritten as:

$$\begin{bmatrix} \Gamma_{smn} & 0 \\ 0 & \Gamma_{smn} \end{bmatrix} \begin{Bmatrix} \ddot{\vec{q}}_{mn}^s(t) \\ \ddot{\vec{q}}_{mn}^c(t) \end{Bmatrix} + 2\Omega n \begin{bmatrix} 0 & -\Gamma_{smn} \\ \Gamma_{smn} & 0 \end{bmatrix} \begin{Bmatrix} \dot{\vec{q}}_{mn}^s(t) \\ \dot{\vec{q}}_{mn}^c(t) \end{Bmatrix} + \begin{bmatrix} \phi_{smn} - \Omega^2 n^2 \Gamma_{smn} & 0 \\ 0 & \phi_{smn} - \Omega^2 n^2 \Gamma_{smn} \end{bmatrix} \begin{Bmatrix} \vec{q}_{mn}^s(t) \\ \vec{q}_{mn}^c(t) \end{Bmatrix} = \frac{1}{\rho h} \begin{Bmatrix} \vec{Q}_{sn}^s \\ \vec{Q}_{sn}^c \end{Bmatrix} \tag{15}$$

Here,  $\Gamma_{smn}$  is a symmetric matrix with  $(M+1) \times (M+1)$  dimensions. Also,  $\phi_{smn}$  is a matrix with  $(M+1) \times (M+1)$  dimensions. Equation (15) can be expressed in short form:

$$\mathbf{M}_n \ddot{\vec{q}}_n(t) + \mathbf{G}_n \dot{\vec{q}}_n(t) + \mathbf{K}_n \vec{q}_n(t) = \vec{Q}_n(t) \tag{16}$$

Here,  $\mathbf{M}_n$ ,  $\mathbf{G}_n$  and  $\mathbf{K}_n$  are the matrices with  $2(M+1) \times 2(M+1)$  dimensions and  $\vec{q}_n(t)$ ,  $\dot{\vec{q}}_n(t)$ ,  $\ddot{\vec{q}}_n(t)$  and  $\vec{Q}_n(t)$  are the vectors with  $2(M+1) \times 1$  dimensions and are given as follows:

$$\mathbf{M}_n = \begin{bmatrix} \Gamma_{smn} & 0 \\ 0 & \Gamma_{smn} \end{bmatrix} \quad \mathbf{G}_n = 2\Omega n \begin{bmatrix} 0 & -\Gamma_{smn} \\ \Gamma_{smn} & 0 \end{bmatrix} \quad \mathbf{K}_n = \begin{bmatrix} \phi_{smn} - \Omega^2 n^2 \Gamma_{smn} & 0 \\ 0 & \phi_{smn} - \Omega^2 n^2 \Gamma_{smn} \end{bmatrix} \tag{17}$$

$$\vec{q}_n(t) = \begin{Bmatrix} \vec{q}_{mn}^s(t) \\ \vec{q}_{mn}^c(t) \end{Bmatrix} \quad \dot{\vec{q}}_n(t) = \begin{Bmatrix} \dot{\vec{q}}_{mn}^s(t) \\ \dot{\vec{q}}_{mn}^c(t) \end{Bmatrix} \quad \ddot{\vec{q}}_n(t) = \begin{Bmatrix} \ddot{\vec{q}}_{mn}^s(t) \\ \ddot{\vec{q}}_{mn}^c(t) \end{Bmatrix} \quad \vec{Q}_n(t) = \begin{Bmatrix} \vec{Q}_{sn}^s \\ \vec{Q}_{sn}^c \end{Bmatrix} \tag{18}$$

$\mathbf{M}_n$  is real, symmetric and positive-definite,  $\mathbf{G}_n$  is real and skew-symmetric and  $\mathbf{K}_n$  is also real and symmetric.  $q_{mn}^s(t)$  and  $q_{mn}^c(t)$  are vectors of generalized coordinates with  $(M+1)$  dimensions.  $\vec{Q}_{sn}^s$  and  $\vec{Q}_{sn}^c$  are vectors of external excitation force with  $(M+1)$  dimensions. External excitation force, which is applied on the disk surface perpendicular, is a time-varying single force:

$$p(r, \psi, t) = \frac{F}{r} \delta(r - R_1) \delta(\psi - \psi_1) \sin(\bar{\omega}t - \phi_1) \tag{19}$$

Here,  $\delta$  is Dirac delta function,  $R_1$  and  $\psi_1$  are excitation coordinates,  $\bar{\omega}$  is the frequency of external excitation force,  $\phi_1$  is the phase angle of the external excitation force. Expressions in right-hand side of Equation (14) can be arranged as follows:

$$\frac{1}{\pi \rho h} \int_{R_i}^{R_o} \int_0^{2\pi} p(r, \psi, t) R_{sn}(r) r \cos n\psi d\psi dr = \frac{1}{\pi \rho h} F R_{sn}(R_1) \cos n\psi_1 \sin(\bar{\omega}t - \phi_1) \tag{20}$$

$$\frac{1}{\pi \rho h} \int_{R_i}^{R_o} \int_0^{2\pi} p(r, \psi, t) R_{sn}(r) r \sin n\psi d\psi dr = \frac{1}{\pi \rho h} F R_{sn}(R_1) \sin n\psi_1 \sin(\bar{\omega}t - \phi_1) \tag{21}$$

Equation (16) can be converted from second order differential equation to two first order differential equations by using the variables consisting of  $\vec{q}_n$  and its derivations below:

$$\vec{x} = \begin{Bmatrix} \vec{q}_n(t) \\ \dot{\vec{q}}_n(t) \end{Bmatrix} \quad \dot{\vec{x}} = \begin{Bmatrix} \dot{\vec{q}}_n(t) \\ \ddot{\vec{q}}_n(t) \end{Bmatrix} \tag{22}$$

Thus, differential equations are obtained in matrix notation as follows:

$$\begin{bmatrix} \mathbf{K}_n & 0 \\ 0 & \mathbf{M}_n \end{bmatrix} \begin{Bmatrix} \dot{\vec{q}}_n(t) \\ \ddot{\vec{q}}_n(t) \end{Bmatrix} + \begin{bmatrix} 0 & -\mathbf{K}_n \\ \mathbf{K}_n & \mathbf{G}_n \end{bmatrix} \begin{Bmatrix} \vec{q}_n(t) \\ \dot{\vec{q}}_n(t) \end{Bmatrix} = \begin{Bmatrix} 0 \\ \vec{Q}_n \end{Bmatrix} \tag{23}$$

In short form, Equation (23) can be rewritten by using Equation (22) as indicated below:

$$\mathbf{M}^* \dot{\vec{x}} + \mathbf{G}^* \vec{x} = \vec{Q}_n^* \quad (24)$$

Here,  $\mathbf{M}^*$  and  $\mathbf{G}^*$  are the matrices with  $4 \times (M+1) \times 4 \times (M+1)$  dimensions and  $\vec{Q}_n^*$  is a vector with  $4 \times (M+1) \times 1$  dimension. The abbreviations can be represented as noted below:

$$\mathbf{M}^* = \begin{bmatrix} \mathbf{K}_n & 0 \\ 0 & \mathbf{M}_n \end{bmatrix} \quad \mathbf{G}^* = \begin{bmatrix} 0 & -\mathbf{K}_n \\ \mathbf{K}_n & \mathbf{G}_n \end{bmatrix} \quad \vec{Q}_n^* = \begin{Bmatrix} 0 \\ \vec{Q}_n \end{Bmatrix} \quad (25)$$

Equation (24) can be written as:

$$\dot{\vec{x}} = \mathbf{A} \vec{x} + \mathbf{B} \quad (26)$$

Here,  $\mathbf{A}$  and  $\mathbf{B}$  matrices are with  $4 \times (M+1) \times 4 \times (M+1)$  dimensions and are given as follows:

$$\mathbf{A} = -(\mathbf{M}^*)^{-1} \mathbf{G}^* \quad \mathbf{B} = (\mathbf{M}^*)^{-1} \vec{Q}_n^* \quad (27)$$

By applying  $\vec{y} = \dot{\vec{x}}$  transformation, Equation (26) can be rewritten as;

$$\vec{y} = \mathbf{C} \vec{x} + \mathbf{D} \quad (28)$$

Here, if  $\vec{y} = \dot{\vec{q}}_n$  transformation is made by using Equation (22),  $\mathbf{C}$  and  $\mathbf{D}$  matrices are obtained.

$$\mathbf{C} = [\mathbf{0} \quad \mathbf{I}] \quad \mathbf{D} = \mathbf{0} \quad (29)$$

Thus, the problem is expressed in state space form.

### 3. RESULTS (POWER SPECTRAL DENSITY DIAGRAMS)

Power spectral density (PSD) function shows the energy density as a function of frequency. In other words, the PSD diagram gives the energy density of the signal for each frequency. In this stage, the numerical results are obtained for some example problems. A rotating disk with dynamic forces applied perpendicular on it is investigated. The geometric and material properties of the disk are chosen as; the inner radius of the disk,  $R_i$ , is 0.024 m; the outer radius,  $R_o$ , is 0.08 m; the thickness of disk,  $h$ , is 1 mm; the density of the disk material,  $\rho$ , is 7850 kg/m<sup>3</sup>; the Young's modulus,  $E$ , is 206 GPa and the Poisson's ratio,  $\nu$ , is 0.3. The rotational speed of the disk,  $\Omega$ , is 192.75 Hz.

In the first example, a single excitation force is applied to the disk surface perpendicularly. The frequency of the excitation force is set to the first mode frequency of the rotating disk and the magnitude of the force is 1 N. Excitation point is 6.6 cm from the center. In Figure 1, PSD diagram for this example is presented. Here, the phase difference that is time delay of the force from the starting time is zero. As it can be seen from Figure 1, since the excitation frequency coincides with the first mode frequency, the amplitude value increased significantly at that frequency, as it is expected.

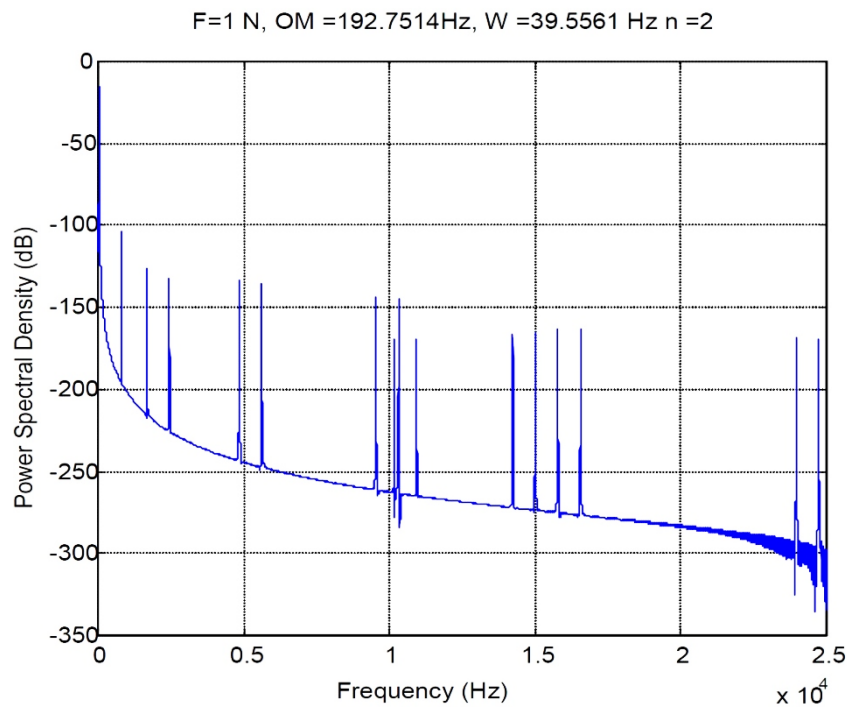


**Figure 1.** PSD diagram for a single excitation force which is set to first mode frequency

As another example, the same case is investigated and at this time, the frequency of the excitation force is set to the third mode frequency of the disk with no phase angle. In Figure 2, the PSD diagram for this case is presented. It is clear that the amplitude at the third mode frequency of the disk is much more greater than those of other frequencies.

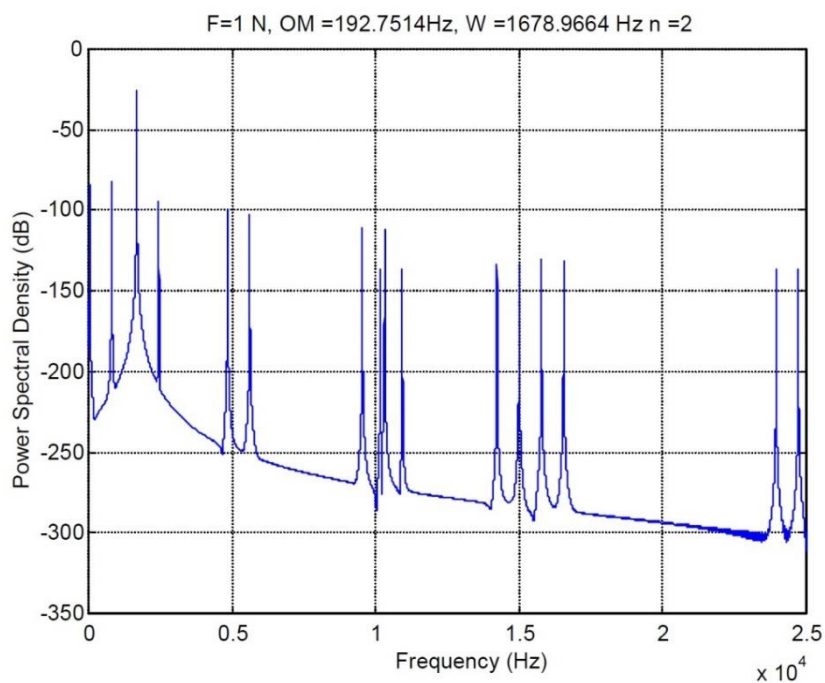


**Figure 2.** PSD diagram for a single excitation force which is set to third mode frequency with zero phase difference

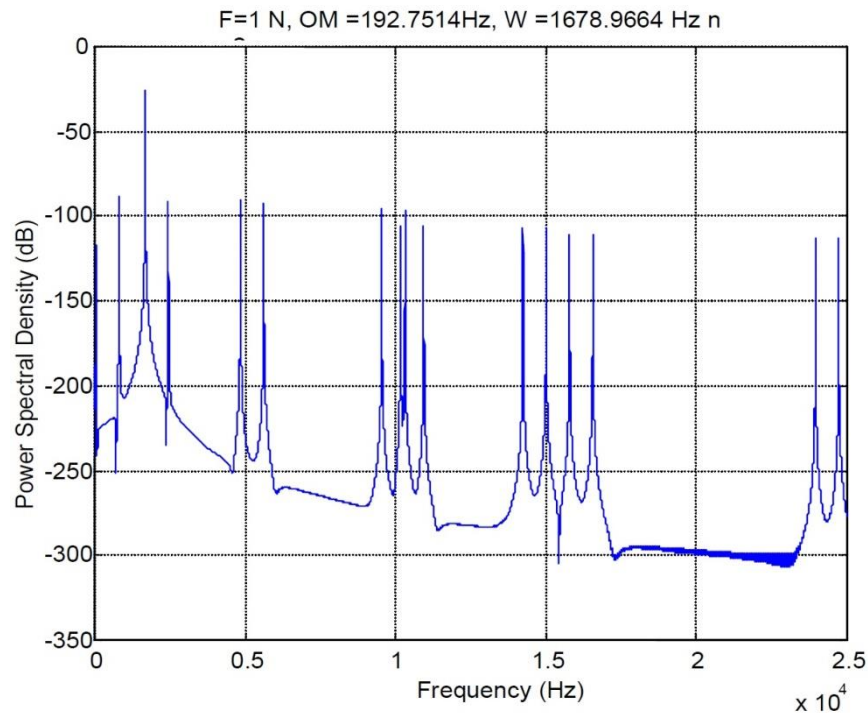


**Figure 3.** PSD diagram for a single excitation force which is set to third mode frequency and phase difference is  $\pi/2$

In another case, Figure 3 gives the PSD diagram of this disk that has  $\pi/2$  phase difference. For various phase difference values, the amplitudes of other modes change comparatively. It can be used to eliminate large amplitudes of some vibrational modes by adjusting the positions, numbers, frequencies and phase differences of the excitation forces.

In Figure 4, two forces, which have 1 N magnitudes, are applied to the disk at different locations. Phase differences of forces are  $\pi/6$ . Excitation points are 6.6 cm from the center. Excitation frequency is set to the first mode frequency of the disk. As it can be seen from the Figure 4, the amplitude value increases considerably at excitation frequency, while those of the other modes relatively decrease. If Figure 4 is compared with Figure 1, it can be seen that the general characteristics of the diagram change and amplitudes of some mode shapes decrease. Therefore, the authors think that undesired amplitudes of a rotating disk can be eliminated or the vibrational characteristics of a rotating disk can be tailored by adjusting the number, positions, frequencies and phase angles of the excitation forces.

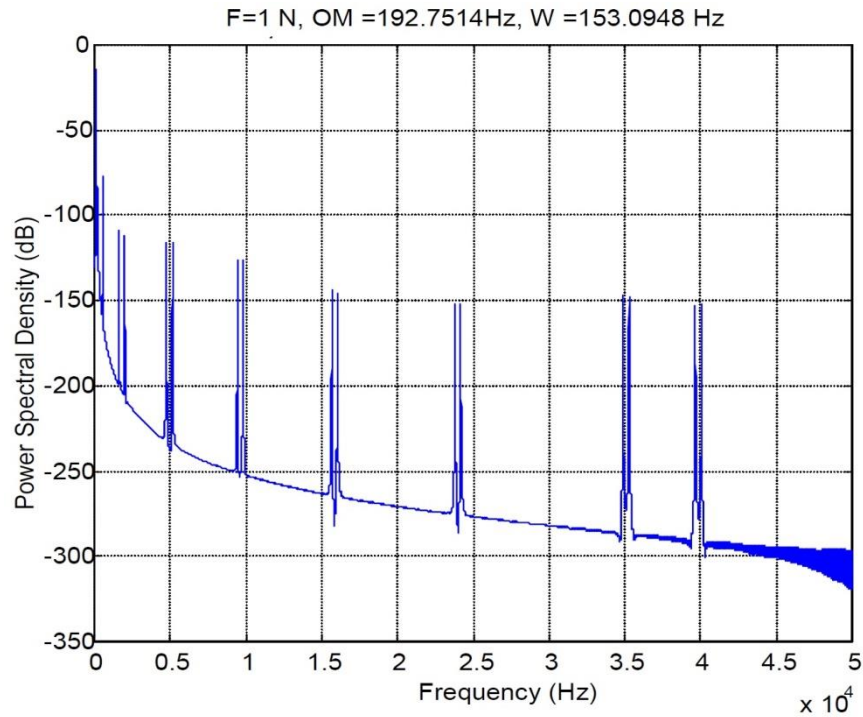


**Figure 4.** PSD diagram for two different excitation forces which have  $\pi/6$  phase difference

Two excitation forces are applied to the rotating disk at different locations and their magnitudes are 1N. The angular positions of the forces are  $\pi/4$  and  $\pi/2$ , and the radial positions are the same; 6.6 cm from the center. The phase angles are  $\pi/2$  and 0. The PSD diagram for this case is given in Figure 5.

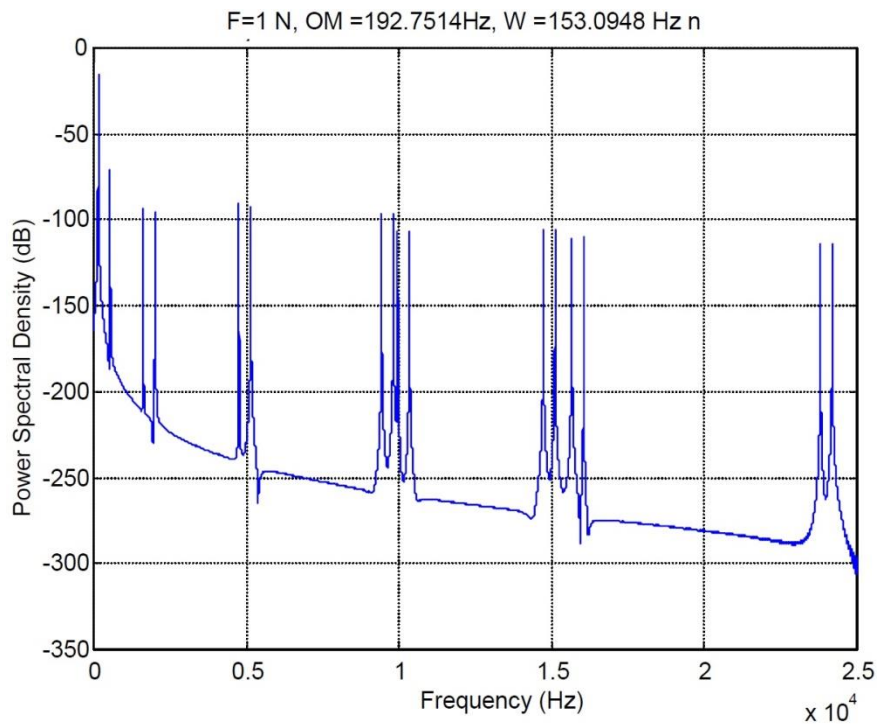


**Figure 5.** PSD diagram for two excitation forces which have different excitation locations and different phase differences

The amplitude of the first mode becomes closer to those of the other modes. This means that the amplitudes of some mode can be reduced considerably, if the excitation force with a proper phase angle is applied to a proper position.

#### 4. CONSLUSIONS

In this study, the forced vibration of the rotating disk is investigated. Excitation forces are applied perpendicular to the rotating disk. The effects of the number, frequencies, phase differences and locations of excitation forces on the modes are investigated. The power densities of the modes are obtained and the PSD diagrams are plotted.

In the literature, mostly, finite element analysis is used to study the forced vibrations of a rotating disk. In this paper, differential equation is solved by using the Galerkin method. Furthermore, in the literature, as far as the authors know, it has not been found any paper studying more than one excitation force. It is thought that vibrations can be controlled effectively by setting the properties and the number of the excitation forces properly. In that kind of control application, a more detailed investigation may be required due to increasing importance of excitation frequencies, excitation locations and phase differences.

It is observed that a force which is set to a specific frequency at any arbitrary excitation location can decrease energies of the amplitudes of some modes. Thus, it is thought that by using a well-designed force system, unwanted vibrations can be eliminated and the vibrational characteristic of a rotating disk may be tailored.

#### CONFLICTS OF INTEREST

No conflict of interest was declared by the authors.

#### REFERENCES

- [1] Lamb, H. and Southwell, R.V., "The vibrations of a spinning disk," *Proceedings of the Royal Society, Series A*, 99: 272-280, (1921).
- [2] Southwell, R.V., "On the free transverse vibrations of a uniform circular disc clamped at its center, and on the effects of rotation," *Proceeding of the Royal Society, Series A*, 101: 133, (1922).
- [3] Kirkhope, J. and Wilson, G.J., "Vibration and stress analysis of thin rotating discs using annular finite elements," *Journal of Sound and Vibration*, 44(4): 461-474, (1976).
- [4] Cole, K.A. and Benson, R.C., "A fast eigenfunction approach for computing spinning disk deflections", *Journal of Applied Mechanics*, 55(2): 453-457, (1986).
- [5] Guven, U., "On transverse vibrations of a rotating disk uniform strength", *Journal of Applied Mechanics*, 59(1): 234-235, (1992).
- [6] Lee, C.W. and Kim, M.E., "Separation and identification of travelling wave modes in rotating disk via directional spectral analysis", *Journal of Sound and Vibration*, 187(5): 851-864, (1995).
- [7] Pei, Y.C. and Tan, Q.C., "Modal interactions in a rotating flexible disc", *Proceedings of the Institution of Mechanical Engineers, Part C: Journal of Mechanical Engineering Science*, 223(4): 851-857, (2009).
- [8] Ramaiah, G.K., "Natural frequencies of spinning annular plates", *Journal of Sound and Vibration*, 74(2): 303-310, (1981).

- [9] Tseng, C.W., Shen, J.Y. and Shen, I.Y., "Vibration of rotating-shaft HDD spindle motors with flexible stationary parts", *IEEE Transactions on Magnetics*, 39(2 I): 794-799, (2003).
- [10] D'Angelo, C. and Mote, C.D., "Natural frequencies of a thin disk clamped by thick collars with friction at the contacting surfaces spinning at high rotation speed", *Journal of Sound and Vibration*, 168(1): 1-14, (1993).
- [11] Tufekci, E. and Oldac, O., "Free and forced vibrations of a rotating elastic disk", *The First International Structural Conference on Stability and Dynamics*, Taipei Taiwan, (2000).
- [12] Honda, Y., Matsuhisa, H. and Sato, S., "Modal response of a disk to a moving concentrated harmonic force", *Journal of Sound and Vibration*, 102(4): 457-472, (1985).
- [13] Weisensel, G.N. and Schlack, A.L., "Response of annular plates to circumferentially and radially moving loads", *Journal of Applied Mechanics*, 60(3): 649-661, (1993).
- [14] Benson, R.C. and Bogy, D.B., "Deflection of a very flexible spinning disk due to a stationary transverse load", *Journal of Applied Mechanics*, 45(3): 636-642, (1978).
- [15] Chen, J.S. and Hsu, C.M., "On the transient response of a spinning disk under a space fixed load", *Journal of Applied Mechanics*, 64(4): 1017-1019, (1997).
- [16] Huang, S.C. and Hsu, B.S., "Vibrations of a spinning annular plate with multi-circular line guides", *Journal of Sound and Vibration*, 164(3): 535-547, (1993).
- [17] Hutton, S.G., Chonan, S. and Lehmann, B.F., "Dynamic response of a guided circular saw", *Journal of Sound and Vibration*, 112(3): 527-539, (1987).
- [18] Chen, J.S., "Vibration and sensitivity analysis of a spinning disk under tangential edge loads", *Journal of Sound and Vibration*, 215(1): 1-15, (1998).
- [19] Iwan, W.D. and Moeller, T.L., "The stability of a spinning elastic disk with a transverse load system", *Journal of Applied Mechanics*, 43(3): 485-490, (1976).
- [20] Adams, G.G., "Critical speeds for a flexible spinning disk", *International Journal of Mechanical Science*, 29(8): 525-531, (1987).
- [21] Ona, K., Chen, J.S. and Bogy, D.B., "Stability analysis for the head-disk interface in a flexible disk drive", *Journal of Applied Mechanics*, 58(4): 1005-1014, (1991).
- [22] Jiang, Z.W., Chonan, S. and Abe, H., "Dynamic response of a read-write head floppy disk system subjected to axial excitation", *Journal of Vibration and Acoustics*, 112(1): 53-58, (1990).
- [23] Ono, K., Maeno, T., Ebihara, T., "Study on mechanical interface between head and media in flexible disk drive", *Bulletin of JSME*, 29(255): 3109-3115, (1986).
- [24] Huang, S.C. and Chiou, W.J., "Modeling and vibration analysis of spinning-disk and moving-head assembly in computer storage systems", *Journal of Vibration and Acoustics*, 119(2): 185-191, (1997).
- [25] Xu, L.M. and Guo, N., "Modal testing and finite element modelling of subsystem in hard disk drive", *Mechanical Systems and Signal Processing*, 17(4): 747-764, (2003).
- [26] Zhang, W. and Yang, X., "Transverse nonlinear vibrations of a circular spinning disk with a varying rotating speed", *Science China Physics, Mechanics, Astronomy*, 53(8): 1536-1553, (2010).

- [27] Younesian, D., Aleghafourian, M.H., Esmailzadeh, E., “Vibration analysis of circular annular plates subjected to peripheral rotating transverse loads”, *Journal of Vibration and Control*, 21(7): 1443-1455, (2013).
- [28] Norouzi, H. and Younesian, D., “Forced vibration analysis of spinning disks subjected to transverse loads”, *International Journal of Structural Stability and Dynamics*, 15(3): 1450049, (2015).